

Qualitative Evaluation of Flight Controller Performances for Autonomous Quadrotors

Aleksandar Rodić, Gyula Mester, and Ivan Stojković

Abstract. The paper regards to benchmarking and qualitative evaluation of different autonomous quadrotor flight controllers. Three characteristic representatives of frequently used flight control techniques are considered: PID, backstepping and fuzzy. The paper aims to contribute to the objective assessment of quadrotor control performances with respect to the criteria regarding to dynamic performances, trajectory tracking precision, energy efficiency and control robustness upon stochastic internal and/or external perturbation. Qualitative evaluation of the closed-loop system performance should enable the best choice of microcopter control structure. Non-linear modeling, control and numerical simulation of two characteristic flight test-scenarios (indoor as well as outdoor) are described in the paper, too. Obtained simulation results for three representative control algorithms are graphically and table presented, analyzed and discussed.

Keywords: Autonomous quadrotor, flight controller, PID controller, fuzzy controller.

1 Introduction

Over the recent years, many research groups are working in order to exploit the potential advantages of quadrotor rotorcrafts as UAVs of future. This paper is addressed to problems of controller performances evaluation and analysis. The main benefits of this research concern with achievement of a controller architecture that

Aleksandar Rodić · Ivan Stojković
Mihajlo Pupin Institute, Robotics Laboratory,
Volgina 15, 11060 Belgrade, Serbia
e-mail: {aleksandar.rodic, ivan.stojkovic}@pupin.rs

Gyula Mester
University of Szeged, Faculty of Engineering,
6725 Szeged, Moszkvai krt. 5-7, Hungary
e-mail: drmestergyula@gmail.com

should enable quadrotor high dynamic performances, robustness to external perturbations as well as satisfactory trajectory tracking precision.

The overview of the most important techniques and the respective publications are listed in the text to follow. The Lyapunov Theory of Stability was frequently considered in the literature as for example [1] - [3]. According to this technique, it is possible to ensure, under certain condition, the asymptotical stability of the micro copter.

The linear control techniques based on proportional-integral-derivative (PID) feedback structure [4], [5] are frequently used with micro copters for flight control. The strength of the PID feedback is the exponential convergence property mainly due to the compensation of the Coriolis and gyroscopic terms. On the contrary a PID structure does not require some specific model parameters and the control law is much simpler to implement.

Some researchers used adaptive techniques [6] [7]. These methods provide good performance with parametric uncertainties and unmodeled dynamics.

The control based on a Linear quadratic Regulator (LQR) [4] [8] [9] shows fine results. The main advantage of this technique is that the optimal input signal turns out to be obtainable from full state feedback (by solving the Ricatti equation). On the other hand the analytical solution to the Ricatti equation is difficult to compute.

In the recent time, very popular control technique is done with backstepping control [10]. In the respective publications the convergence of the quadrotor internal states is guaranteed, but a lot of computation is required.

Dynamic control methods are based on use of a dynamic feedback [11] [12]. This technique is implemented in few quadrotor projects to transform the closed loop part of the system into a linear, controllable and decoupled subsystem.

There are also control methods based on utilization of visual feedback information. The camera used for this purpose can be mounted on-board [13] [14] (fixed on the helicopter) or off-board [15] [16] (fixed to the ground).

Other control algorithms belong to the class so called the knowledge-based algorithms. Main characteristics of these methods are that they represent non-linear techniques that do not require knowledge about the model of system. These techniques assume quadrotor plant as a black-box. They use control platform with fuzzy techniques [17], neural networks [18] and reinforcement learning [19].

In [20] a procedure allowing the computation of time-optimal quadrotor maneuvers for arbitrary initial and final states by solving the boundary value problem induced by the minimum principle. The algorithm allows the computation of quadrotor maneuvers that satisfy Pontryagins minimum principle with respect to time-optimality. Such maneuvers provide a useful lower bound on the duration of maneuvers, which can be used to assess performance of controllers and vehicle design parameters. The usage of the computed maneuvers as a benchmark is demonstrated by evaluating quadrotor design parameters, and a linear feedback control law as an example of a control strategy.

The main contribution of the paper regards to design and simulation of the appropriate simulation benchmark procedures (indoor as well outdoor) to be used for the objective assessment and evaluation of different control algorithms applied to microcopoter rotorcrafts.

2 Quadrotor Dynamics Modeling

The quadrotor is satisfactory well modeled [21] - [23] with a four rotors in a cross configuration Fig. 1. This cross structure is quite thin and light, however it shows robustness by linking mechanically the motors (which are heavier than the structure). Each propeller is connected to the motor through the reduction gears. All the propellers axes of rotation are fixed and parallel. Furthermore, they have fixed-pitch blades and their air flows point downwards (to get an upward lift). These considerations point out that the structure is quite rigid and the only things that can vary are the propeller speeds.

As shown in Fig. 1, one pair of opposite propellers of quadrotor rotates clockwise (2 and 4), whereas the other pair rotates anticlockwise (1 and 3). This way it is able to avoid the yaw drift due to reactive torques. This configuration also offers the advantage of lateral motion without changing the pitch of the propeller blades. Fixed pitch simplifies rotor mechanics and reduces the gyroscopic effects. Control of quadrotor is achieved by commanding different speeds to different propellers, which in turn produces differential aerodynamic forces and moments. For hovering, all four propellers rotate at same speed. For vertical motion, the speed of all four propellers is increased or decreased by the same amount, simultaneously. In order to pitch and move laterally in that direction, speed of propellers 3 and 1 is changed conversely. Similarly, for roll and corresponding lateral motion, speed of propellers 2 and 4 is changed conversely. To produce yaw, the speed of one pair of two oppositely placed propellers is increased while the speed of the other pair is decreased by the same amount. This way, overall thrust produced is same, but differential drag moment creates yawing motion. In spite of four actuators, the quadrotor is still an under-actuated system.

The Fig. 1 shows the structure model [22] [23] in hovering condition, where all the propellers have the same speed of rotation $\omega_i = \omega_H$, $i = 1, \dots, 4$. In the Fig. 1 all the propellers rotate at the same (hovering) speed ω_H (rad/s) to counterbalance the acceleration due to gravity. Thus, the quadrotor performs stationary flight and no forces or torques moves it from its position. Even though, the quadrotor has 6 DOFs, it is equipped just with four propellers hence it is not possible to reach a desired set-point for all the DOFs, but at maximum four. However, thanks to its structure, it is quite easy to choose the four best controllable variables and to decouple them to make control easier. The four quadrotor targets are thus related to the four basic movements which allow the microcopter to reach a certain height and attitude.

To describe the motion of a 6 DOF rigid body it is usual to define two reference frames Fig. 1 : (i) the earth inertial frame (E-frame), and (ii) the body-fixed frame (B-frame).

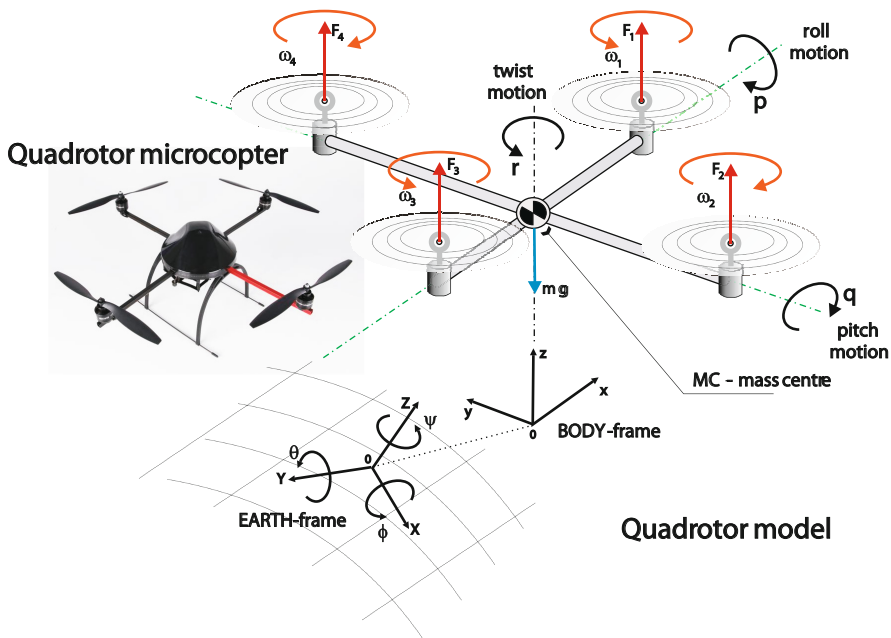


Fig. 1 Quadrotor rotorcraft – a non-linear dynamic system that uses synergy of its rotary-wings to fly. Commonly used model of quadrotor with corresponding degrees of freedom. Coordinate systems assumed to enable model derivation.

The linear position of the helicopter (X, Y, Z) is determined by the coordinates of the vector between the origin of the B-frame and the origin of the E-frame according to equation. The angular position (or attitude) of the helicopter (φ, θ, ψ) is defined by the orientation of the B-frame with respect to the E-frame. The vector that describes quadrotor position and orientation is:

$$s = [X \ Y \ Z \ \varphi \ \theta \ \psi]^T. \quad (1)$$

The generalized quadrotor velocity expressed in the B-frame can be written as [1]:

$$v = [u \ v \ w \ p \ q \ r]^T, \quad (2)$$

where, the u, v, w represent linear velocity components in the B-frame, while p, q, r are corresponding angular velocities of rotation about corresponding roll, pitch and yaw axes. Finally, the kinematical model of the quadrotor correlates the motions in these two coordinate systems [21].

The quadrotor dynamics can be described in the known form [21], extended by adding of the air-resistance member. The equation that describes model in B-frame is:

$$M_B \dot{v} + C_B(v)v + G_B(s) + R_a(v) = O_B(v)\Omega + E_B\Omega^2, \quad (3)$$

where \dot{v} is the generalized acceleration vector with respect to (w.r.t.) the B-frame, M_B is the system inertia matrix, C_B is the Coriolis-centripetal matrix and G_B is the gravitational force vector, all expressed w.r.t. the B-frame. The R_a is the air-resistance vector. The O_B and E_B are the gyroscopic propeller matrix and the movement matrix, successively. The gyroscopic propeller matrix O_B depends on total rotational moment of inertia around the propeller axis and corresponding angular speeds p , q . The matrix E_B depends on the design parameters – thrust and drag coefficients. Air resistance forces appear as an external perturbation to the quadrotor translational movements in longitudinal (x), lateral (y) and normal (z) direction w.r.t B-frame. The drag force R_a depends on a magnitude of body-fluid relative velocity. It takes into account both - air resistance and wind gust.

$$R_a = \frac{1}{2}\rho \cdot \begin{bmatrix} (\dot{x} - v_{w,x})^2 \cdot C_{d,x} \cdot A_x \\ (\dot{y} - v_{w,y})^2 \cdot C_{d,y} \cdot A_y \\ (\dot{z} - v_{w,z})^2 \cdot C_{d,z} \cdot A_z \end{bmatrix} \quad (4)$$

In equation (4) ρ is the air density, $C_{d,x}$, $C_{d,y}$ and $C_{d,z}$ are drag coefficients, A_x , A_y , A_z are reference areas exposed against the streaming fluid, $v_{w,x}$, $v_{w,y}$, $v_{w,z}$ are wind velocity components in the particular directions w.r.t B-frame.

Equation (3), after certain rearrangement and transformation from the B-frame space to E-frame space, can be written in the scalar form suitable for controller design. Now, the model of quadrotor dynamics can be described by a system of equations [21]:

$$\begin{aligned} \ddot{X} &= (\sin \psi \sin \phi + \cos \psi \sin \theta \cos \phi) \frac{U_1}{m} - \frac{R_{a,x}}{m}, \\ \ddot{Y} &= (-\cos \psi \sin \phi + \sin \psi \sin \theta \cos \phi) \frac{U_1}{m} - \frac{R_{a,y}}{m}, \\ \ddot{Z} &= -g + \cos \theta \cos \phi \frac{U_1}{m} - \frac{R_{a,z}}{m}, \\ \ddot{\phi} &= \frac{I_{YY} - I_{ZZ}}{I_{XX}} \dot{\theta} \dot{\psi} - \frac{J_{TP}}{I_{XX}} \dot{\theta} \Omega_r + \frac{U_2}{I_{XX}}, \\ \ddot{\theta} &= \frac{I_{ZZ} - I_{XX}}{I_{YY}} \dot{\phi} \dot{\psi} + \frac{J_{TP}}{I_{YY}} \dot{\phi} \Omega_r + \frac{U_3}{I_{YY}}, \\ \ddot{\psi} &= \frac{I_{XX} - I_{YY}}{I_{ZZ}} \dot{\phi} \dot{\theta} + \frac{U_4}{I_{ZZ}}, \end{aligned} \quad (5)$$

where the propeller's speed inputs are given through equation (6) [21]:

$$\underline{U} = \begin{bmatrix} U_1 \\ U_2 \\ U_3 \\ U_4 \end{bmatrix} = \begin{bmatrix} b (\omega_1^2 + \omega_2^2 + \omega_3^2 + \omega_4^2) \\ lb (-\omega_2^2 + \omega_4^2) \\ lb (-\omega_1^2 + \omega_3^2) \\ d (-\omega_1^2 + \omega_2^2 - \omega_3^2 + \omega_4^2) \end{bmatrix} \quad (6)$$

The movement vector \underline{U} in (6) relates to the movement force and torques acting in quadrotor body MC. The component U_1 acts along the z -axis of the B-frame while the movement torques U_2, U_3, U_4 act about the particular B-frame axes - roll, pitch and yaw. The overall propeller's speed Ω_r (rad/s) is defined by equation (7):

$$\Omega_r = -\omega_1 + \omega_2 - \omega_3 + \omega_4. \quad (7)$$

Quadrotor is equipped with four fixed-pitch rotors, each one includes a Brush-Less Direct Current (BLDC) motor, a one-stage gearbox and a rotary-wing (propeller). The entire rotor dynamics can be approximated by a first order transfer function, sufficient to reproduce the dynamics between the propeller's speed set-point and its true speed. The model form is given in (8) [21]:

$$G_m(s) = \frac{K_m}{T_ms + 1} \cdot e^{-\tau_ms}, \quad (8)$$

where K_m , T_m and τ_m are corresponding motor parameters related to gain, time constant and time delay.

3 Control System Architecture

Commonly used control system architecture of autonomous quadrotor microcopter is presented in Fig. 2 [21] [24] [25]. The task planning block is in debt to determine referent 3D rotorcraft trajectory as well as to propose the referent flight speed along the trajectory. The task planning block generates referent path based on flight parameters and microcopter task imposed.

Position control block Fig. 2 has to ensure accurate 3D trajectory tracking. It represents so called outside control loop. Based on sensory information (GPS, IR, SONAR) about the referent positions (speeds) and corresponding actual ones defined in the inertial coordinate system (E-frame), the position controller calculates referent attitude position of quadrotor body (pitch θ_{ref} and roll angle φ_{ref}) that have to enable desired motion.

Inner control block represents the core of the control scheme. It is responsible for the attitude control of quadrotor system. Appropriate attitude control ensures in an indirect way required flight performances in the particular directions of motion such as longitudinal, lateral as well as vertical. Inner control block processes the task and sensor data and provides a signal for basic movements which balances the position error. Equation (9) is used in this block to transfer an acceleration command to a basic movement one. The control rules to be used to estimate the acceleration commands are to be considered in the next section.

The essence of building control scheme presented in Fig. 2 is that by controlling a body attitude (within an inner loop) it is enabled controlling of the linear rotorcraft movements. Also, high robustness to parameter and structural uncertainties of system modeling are required in design of attitude control algorithm.

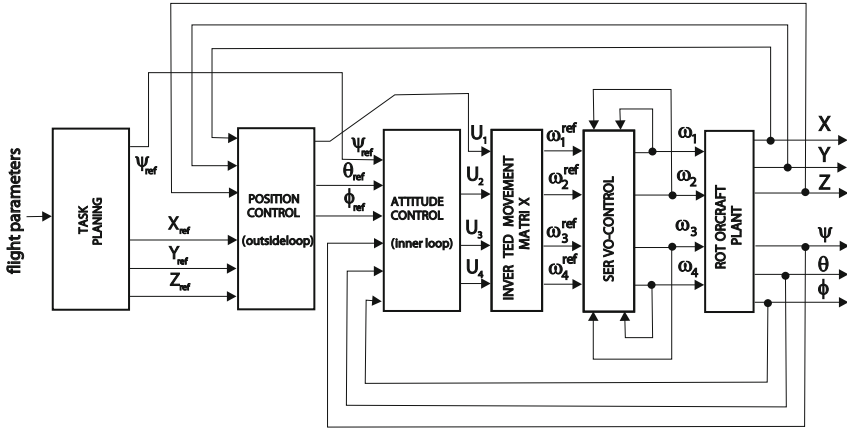


Fig. 2 Block-scheme of the global control system architecture of autonomous UAVs

Inverted Movements Matrix block Fig. 2 is used to compute the propeller's squared speed from the four basic movement signals. Since the determinant of the movement matrix is different than zero, it can be inverted to find the vector Ω^2 . The computation block is shown in equation (9) [21] [24].

$$\Omega^2 = \begin{bmatrix} \omega_1^2 \\ \omega_2^2 \\ \omega_3^2 \\ \omega_4^2 \end{bmatrix}_{ref} = \begin{bmatrix} \frac{1}{4b}U_1 - \frac{1}{2bl}U_3 - \frac{1}{4d}U_4 \\ \frac{1}{4b}U_1 - \frac{1}{2bl}U_2 + \frac{1}{4d}U_4 \\ \frac{1}{4b}U_1 + \frac{1}{2bl}U_3 - \frac{1}{4d}U_4 \\ \frac{1}{4b}U_1 + \frac{1}{2bl}U_2 + \frac{1}{4d}U_4 \end{bmatrix} \quad (9)$$

Variety of control algorithms can be implemented within the flight controller presented in Fig. 2. This paper aims to propose corresponding testing procedure and a qualitative evaluation of three representative flight control techniques. These are: (i) conventional linear PID regulator, (ii) non-linear, model-based backstepping method (BSM), and (iii) non-linear, knowledge-based fuzzy logic control (FLC) based on use of a Fuzzy Inference System. The choice was made due to the reason that the fore mentioned control algorithms are frequently used in the open literature. The PID controller is assumed as the main representative of the linear control techniques. The backstepping method was considered in the paper as a typical representative of the model-based, dynamic, non-linear control method while the fuzzy controller was assumed as the representative of so called knowledge-based control algorithms.

3.1 PID Controller

A proportional-integrative-derivative controller (PID) is most common feedback form in all kinds of control systems, and is also being used for flight control of quadrotor [4] [5]. The ideal PID is represented in continuous time domain as:

$$u(t) = k_P e(t) + k_I \int_0^t e(\tau) d\tau + k_D \frac{de(t)}{dt}, \quad (10)$$

where the terms k_P , k_I and k_D are proportional, integral and derivative gain, respectively, $u(t)$ is the output of the controller, and input $e(t)$, is the reference tracking error. The PID quadrotor flight controller consists of six PID controllers for the particular state coordinates (1), see Fig. 1.

3.2 Backstepping Controller

The backstepping technique is recursive design methodology that makes use of Lyapunov stability theory to force the system to follow a desired trajectory. Backstepping approach to quadrotor flight control was successfully applied in number of researches such as for example [10] [24].

First, the dynamical model from (5) is rewritten in state-space form $\dot{X} = f(X, U)$, by introducing $X = [x_1, \dots, x_{12}]^T \in \mathbb{R}^{12}$ as space vector of the system (7) [24]:

$$\begin{aligned} x_1 &= \phi, & x_5 &= \psi, & x_9 &= Y, \\ x_2 &= \dot{\phi}, & x_6 &= \dot{\psi}, & x_{10} &= \dot{Y}, \\ x_3 &= \theta, & x_7 &= X, & x_{11} &= Z, \\ x_4 &= \dot{\theta}, & x_8 &= \dot{X}, & x_{12} &= \dot{Z}. \end{aligned} \quad (11)$$

Next, the x - coordinates are transformed into the new z - coordinates by means of a diffeomorphism [24].

$$\begin{aligned} z_1 &= x_{1_ref} - x_1, & z_7 &= x_{7_ref} - x_7, \\ z_2 &= x_2 - \dot{x}_{1_ref} - \alpha_1 z_1, & z_8 &= x_8 - \dot{x}_{7_ref} - \alpha_7 z_7, \\ z_3 &= x_{3_ref} - x_3, & z_9 &= x_{9_ref} - x_9, \\ z_4 &= x_4 - \dot{x}_{3_ref} - \alpha_3 z_3, & z_{10} &= x_{10} - \dot{x}_{9_ref} - \alpha_9 z_9, \\ z_5 &= x_{5_ref} - x_5, & z_{11} &= x_{11_ref} - x_{11}, \\ z_6 &= x_6 - \dot{x}_{5_ref} - \alpha_5 z_5, & z_{12} &= x_{12} - \dot{x}_{11_ref} - \alpha_{11} z_{11}. \end{aligned} \quad (12)$$

Introducing the partial Lyapunov functions (example for z_1 and z_2) $V_1(z_1) = \frac{1}{2}z_1^2$ and $V_2(z_1, z_2) = \frac{1}{2}(z_1^2 + z_2^2)$, it is possible to determine the control law such that $\dot{V}_2 < 0$ and therefore the global asymptotic stability will be guaranteed, according to Lyapunov stability theorem, and x_1 tends to x_{1_ref} . Applying this procedure to all x - coordinates results in the following backstepping controller (9):

$$\begin{aligned}
U_X &= \frac{m}{U_1} (z_7 - \alpha_7(z_8 + \alpha_7 z_7) - \alpha_8 z_8), \\
U_Y &= \frac{m}{U_1} (z_9 - \alpha_9(z_{10} + \alpha_9 z_9) - \alpha_{10} z_{10}), \\
U_1 &= \frac{m}{\cos x_1 \cos x_3} (z_{11} + g - \alpha_{11}(z_{12} + \alpha_{11} z_{11}) - \alpha_{12} z_{12}), \\
U_2 &= I_{XX} (z_1 - \frac{I_{YY} - I_{ZZ}}{I_{XX}} x_4 x_6 + \frac{J_{TP}}{I_{XX}} x_4 \Omega_r - \alpha_1(z_2 + \alpha_1 z_1) - \alpha_2 z_2), \\
U_3 &= I_{YY} (z_3 - \frac{I_{ZZ} - I_{XX}}{I_{YY}} x_2 x_6 - \frac{J_{TP}}{I_{YY}} x_2 \Omega_r - \alpha_3(z_4 + \alpha_3 z_3) - \alpha_4 z_4), \\
U_4 &= I_{ZZ} (z_5 - \frac{I_{XX} - I_{YY}}{I_{ZZ}} x_2 x_4 - \alpha_5(z_6 + \alpha_5 z_5) - \alpha_6 z_6),
\end{aligned} \tag{13}$$

where $\alpha_{1,2,\dots,12} > 0$ are parameters of the backstepping flight controller.

3.3 Fuzzy Controller

While some conventional control methods heavily depends on the exact model of controlled system, fuzzy controllers can be designed intuitively in light of the knowledge acquired on the behaviour of the system. This knowledge is often gained through experience and common sense, regardless of the mathematical model of the dynamics governing its behaviour, and it is in the form of set of rules that tries to mimic human-like reasoning. In [25] a Mamdani type of fuzzy inference is used to control quadrotor, and in [26] the comparison of Mamdani and Takagi-Sugeno-Kang (TSK) fuzzy controllers is conducted. The controller that will be implemented here consists of six FLCs, one for each particular state (1), that are in form of zero order TSK fuzzy inference system (14):

$$u = FLC(e, \dot{e}) = \frac{\sum_{k=1}^n \mu_{k,1}(e) \cdot \mu_{k,2}(\dot{e}) \cdot C_k}{\sum_{k=1}^n \mu_{k,1}(e) \cdot \mu_{k,2}(\dot{e})}. \tag{14}$$

FLC described in (14) works with error e and the error rate \dot{e} . Actually, inputs in the FLC are first preprocessed, then they are normalized to fit membership function intervals $[-1 \ 1]$ and $[-3 \ 3]$, and finally feed to FLC. The output of the FLC is control action u . Each input variable possess the corresponding three fuzzy sets NEGATIVE, ZERO and POSITIVE and they are presented in Fig. 3. Output membership functions are fuzzy singletons $C_N = -1$, $C_Z = 0$ and $C_P = 1$.

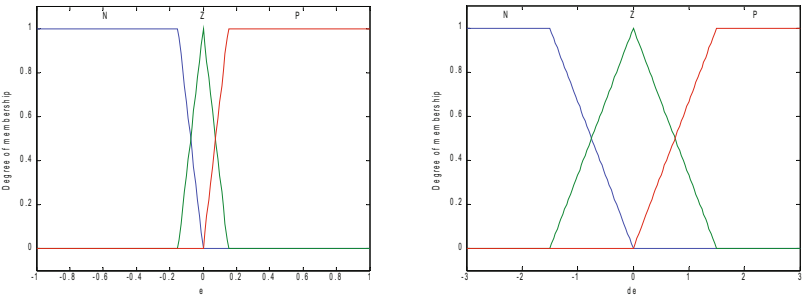


Fig. 3 Membership functions for input variables

Fuzzy rules are in the form: If (e is $\mu_{k,1}$) and (\dot{e} is $\mu_{k,2}$) then (u is C_k), and there are nine rules in the Fuzzy Rule Base that are presented in Table 1.

Table 1 Table of fuzzy rules used for the flight control of quadrotor

Fuzzy rule base			
Rule No	Input e	Input \dot{e}	Output u
1	NEGATIVE	NEGATIVE	NEGATIVE
2	NEGATIVE	ZERO	NEGATIVE
3	NEGATIVE	POSITIVE	ZERO
4	ZERO	NEGATIVE	NEGATIVE
5	ZERO	ZERO	ZERO
6	ZERO	POSITIVE	POSITIVE
7	POSITIVE	NEGATIVE	ZERO
8	POSITIVE	ZERO	POSITIVE
9	POSITIVE	POSITIVE	POSITIVE

4 Simulation Experiments and Flight Controller Evaluation

For the purpose of testing flight controller the following quadrotor parameters are assumed Table 2, [22] [23]. The parameters fit the model described in Sect. 2.

For the purpose of analysis and qualitative evaluation of quadrotor flight controller performances, three representative control algorithms (PID, BSM and FLC) are considered. Control parameters of the PID regulator and Backstepping controller are given in Tables 3 and 4. Fuzzy control parameters are given in Sect. 3.3. Control parameters from Tables 3 and 4 are determined by simulation.

Table 2 Quadrotor model parameters used in simulation experiments

Model parameters					
Symbol	Value	Unit	Symbol	Value	Unit
m	1.0	kg	ρ	1.225	kg/m ³
I_{XX}, I_{YY}	$8.1 \cdot 10^{-3}$	Nms ²	A_x, A_y	0.0121	m ²
I_{ZZ}	$14.2 \cdot 10^{-3}$	Nms ²	A_z	0.0143	m ²
b	$54.2 \cdot 10^{-6}$	Ns ²	$C_{d,x}, C_{d,y}$	1.125	—
d	$1.1 \cdot 10^{-6}$	Nms ²	$C_{d,z}$	1.04	—
l	0.24	m	K_m	0.973	—
J_{TP}	$104 \cdot 10^{-6}$	—	T_m	0.113	—
g	9.81	m/s ²	τ_m	0.112	s

Table 3 PID regulator parameters used in simulation

PID gains	State coordinates $i=1, \dots, 6$					
	1	2	3	4	5	6
proportional	2.22	1.84	1.90	0.30	0.30	0.48
integral	0.01	0.01	0.01	0.20	0.20	0.000001
differential	3.42	2.54	2.28	0.10	0.10	0.04

Table 4 Backstepping controller parameters used in simulation

α_1	α_2	α_3	α_4	α_5	α_6	α_7	α_8	α_{91}	α_{10}	α_{11}	α_{12}
10.7	2.0	9.5	3.8	2.2	2.1	2.0	3.0	2.0	3.0	3.0	3.0

Assessment and qualitative evaluation of three representative control techniques frequently used with UAV are accomplished upon the criteria imposed. The following criteria are introduced: (i) criterion on fine dynamic performances; (ii) criterion on trajectory tracking accuracy; (iii) criterion on control robustness upon the external perturbation; and (iv) criterion on energy efficiency. Control algorithms chosen are evaluated by comparison of the simulation results obtained for the same control object and same flight conditions. Two experimental scenarios are considered as the characteristic benchmarking procedures. These are: (i) dynamic quadrotor flight in the 3D-loop manoeuvre, and (ii) typical cruising flight along the trajectory introduced by setting waypoints with the pre-defined GPS coordinates. Chosen benchmarking tests enable credible assessment of different control techniques under the same conditions.

Dynamic quadrotor flight regards to a microcopter movement in the perpendicular planes in a rather narrow space Fig. 4. It is accomplished by flying in the 3D-loop about a horizontal and a vertical rod set in such a way to be 2 meters far one from another. The curve-linear, smooth loop (trajectory) is pre-defined by introducing 8 key-waypoints Fig. 4. The trajectory defined includes several flight maneuvers: (i) throttle movements in the vertical direction (1-2 and 7-8), (ii) counter-clockwise roll movements (2-3-4 and 5-6-7), (iii) tilt movement about the pitch axis (4-5), and short (iv) hovering with the constant propeller speed (in the point 2 i.e. 7). Quadrotor is required to track the imposed trajectory-loop shown in Fig. 4 moving along at a low speed of maximal value 0.5 (m/s) and to repeat the same path for 33% increased average speed with maximum of 1 (m/s) . Flying in the loop, quadrotor is subjected to influence of the inertia and centripetal forces that tend to run a rotorcraft away from the desired path as well as to disturb its dynamic performances (keeping attitude within the allowed range, smooth acceleration profile, no vibration and turbulence, etc.). The obtained simulation results for the three representative control techniques chosen are summarized, analyzed and commented in the text to follow.

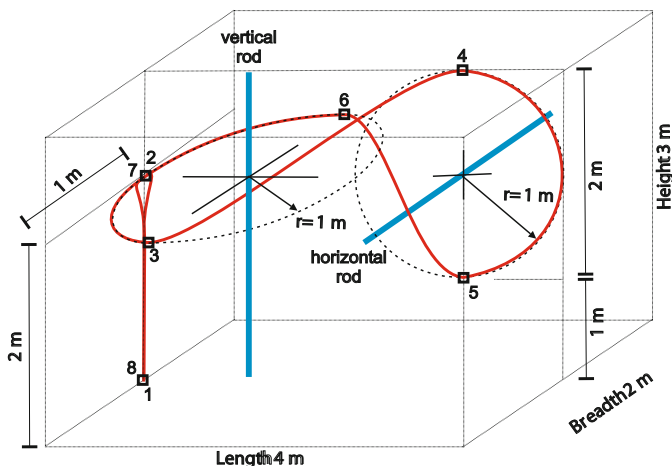


Fig. 4 Trajectory-loop for testing of quadrotor dynamic flight performances

Analyzing the simulation results, Backstepping method ensures the best control performances in sense of trajectory tracking precision. Other two concurrent algorithms have slightly better characteristics in sense of energy efficiency (less consumptions). By increasing of flight speed dynamic effects become influential upon the system performances. Consequently, Backstepping method is more sensitive to changing of flight speed than other two controllers PID and FLC. Degradation of control system performances with excitation of dynamic modes in the case of BSM implementation are shown in Figs. 5 and 6.

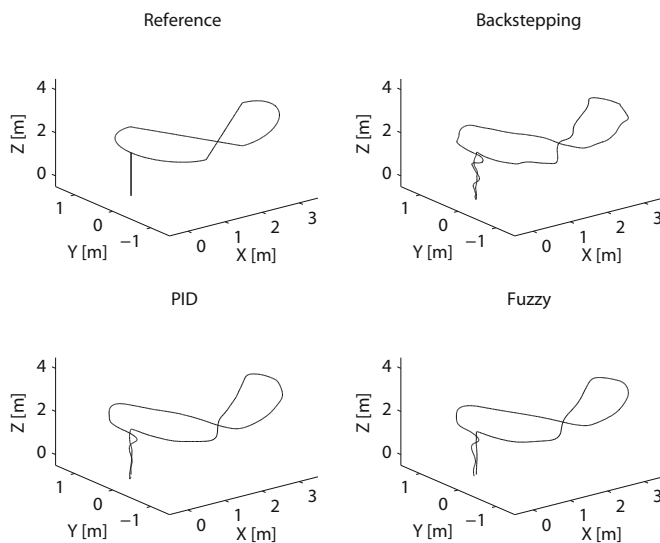


Fig. 5 Trajectory tracking accuracy of the reference path obtained for three examined control techniques and for the case of low speed flight

Corresponding position error in X-, Y-, Z- and Yaw-direction for the “increased” experimental flight speeds is presented in Fig. 7. Corresponding attitude deflections in the roll and pitch directions are shown in Fig. 8.

The second benchmarking procedure (test) considered in the paper regards to assessment of control techniques synthesized to navigate quadcopter towards pre-defined waypoints where the microcopter trajectory is imposed by setting of the reference waypoints whose GPS coordinates (longitude, latitude and altitude) are acquired by use of the Google Earth software [27], Fig. 9.

A multi-segment trajectory of 5689 (*m*) is chosen as test trajectory. It is defined by the 7 waypoints (1-8-3-4-12-10-28-1) whose coordinates are presented in Table 6. Quadcopter is required to track the trajectory by constant cruising speed of 5 (*m/s*). When approaching the particular waypoints, quadcopter varies its flight speed, slows down in order to avoid large deviations of position from the reference path due to inertial effects that become rather expressed especially at high speeds of flight.

Control algorithms PID, BSM and FLC are tested upon the criteria regarding trajectory tracking accuracy, energy efficiency and control robustness upon the internal and external perturbations. In this case, a sudden wind gust is considered as an external perturbation while sensor noise is considered as internal perturbation of the system. Side wind gust is modelled in the paper as additional air-resistance force produced at the quadrotor body due to air streaming (wind blowing). It is assumed the case of south-east wind (143 degrees w.r.t. longitudinal axis) blowing with a constant speed amplitude of 18 (*km/h*).

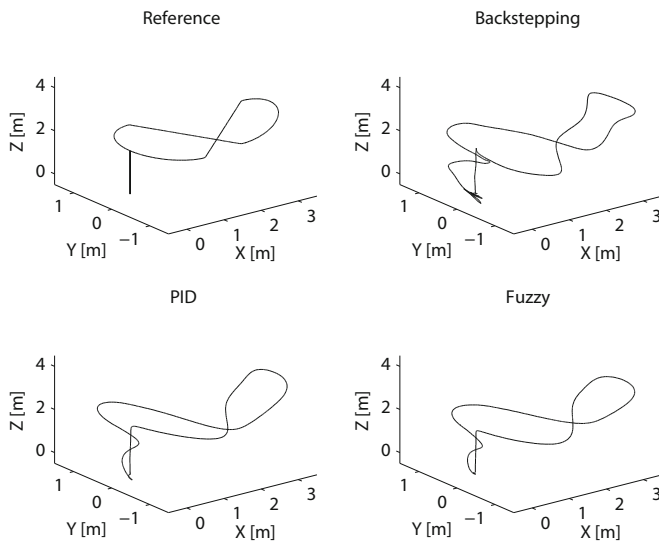


Fig. 6 Trajectory tracking accuracy of the reference path obtained for three considered control techniques and for the case of increased flight speed

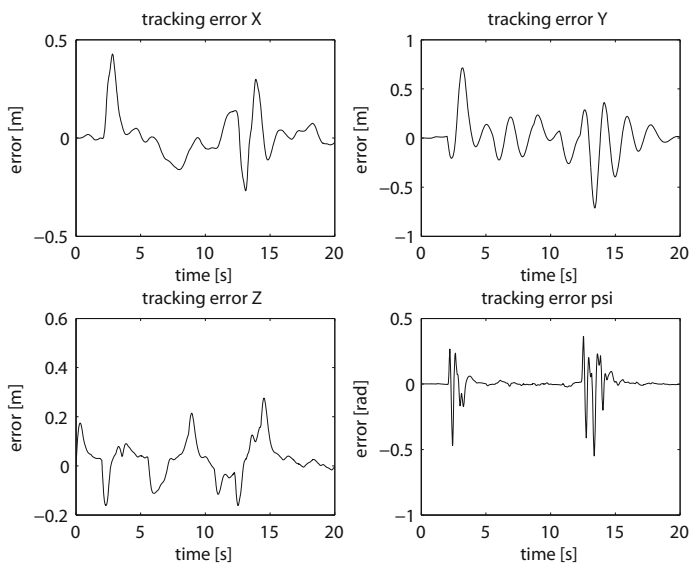


Fig. 7 Position error indicators obtained for the increased flight speed and BSM controller

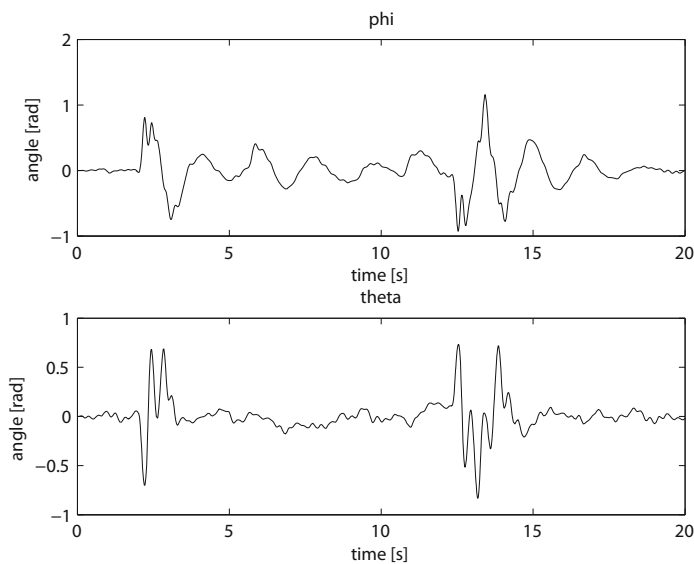


Fig. 8 Attitude deflection (roll and pitch angles) obtained for the increased flight speed and BSM

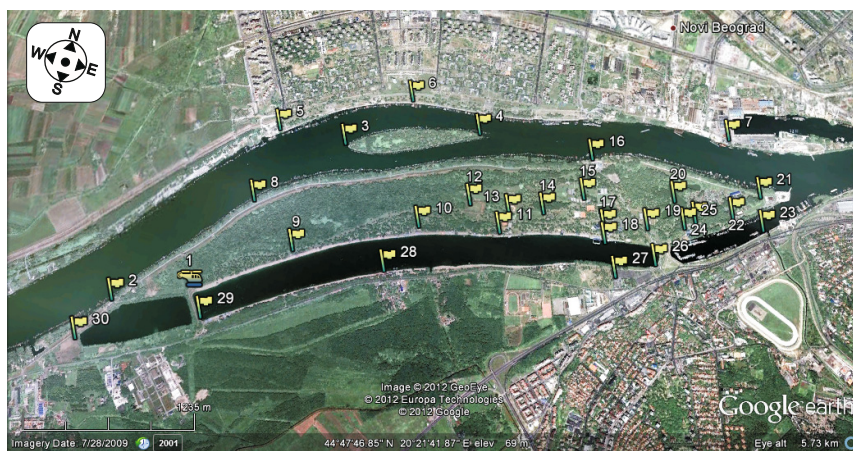


Fig. 9 Fragment of the Google-Earth map [27]. The site “ADA” park of nature (Belgrade, Serbia). Flags in the map are set to mark the particular waypoints used to plot a contour of the desired path model

Table 5 Performance indicators of quadrotor controllers for outdoor flight test scenario

	Perturbation	PID maxi- mal/average	VBSM maxi- mal/average	VFLC maxi- mal/average
Flight duration (s)	noise wind	1172.00 1172.20	1172.30 1172.35	1175.70 1178.30
Energy consump- tions (J)	noise wind	50765 56930	52475 56936	50836 57122
Position error w.r.t. reference trajct. (m)	noise wind	5.55 / 1.57 7.15 / 1.85	5.035 / 1.45 5.46 / 1.558	8.32 / 2.87 16.03 / 3.99
Deviation from the reference altitude (m)	noise wind	0.15 / 0.0326 0.035 / 0.0041	0.35 / 0.0698 0.015 / 0.0001	0.205 / 0.0305 0.154 / 0.0022

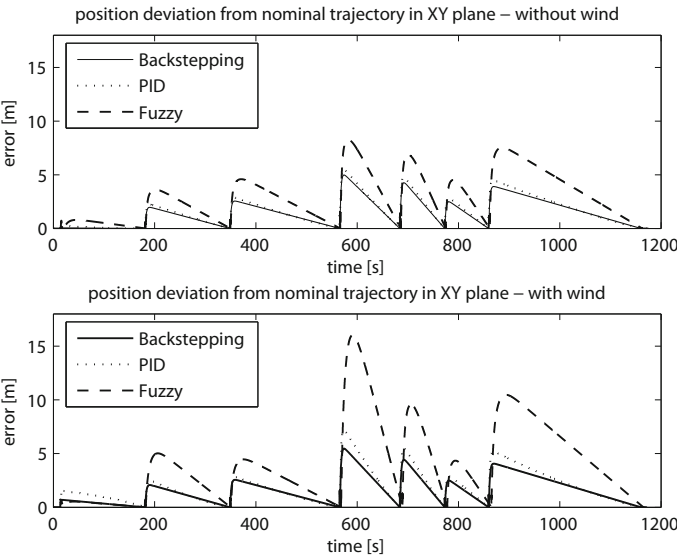


Fig. 10 Trajectory tracking accuracy obtained for implementation of the PID, BSM and FLC controllers in the cases without and with presence external perturbation

Investigating the simulation results reviewed in Table 5, the Backstepping method achieves better control performances than the concurrent PID and FLC controllers bearing in mind the criterion on tracking accuracy. The BSM control shows satisfactory robustness to a side wind gust as external perturbation, too. PID method, as a representative linear technique, achieves satisfactory precision of tracking and better efficiency regarding energy criterion. PID and BSM controllers enable better

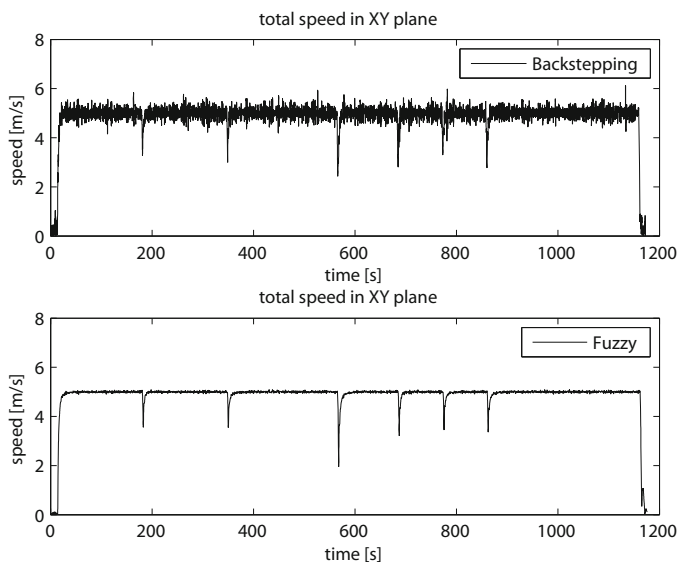


Fig. 11 Flight speed obtained for implementation of the backstepping and fuzzy controller

Table 6 GPS coordinates of the waypoints of the experimental test trajectory 1-8-3-4-12-10-28-1 shown in Fig. 9

Point number	Latitude	Longitude	Altitude (m)
1	44° 46' 40.82''	20° 22' 21.21''	72
3	44° 47' 26.61''	20° 22' 57.66''	67
4	44° 47' 38.12''	20° 23' 14.35''	67
8	44° 47' 06.30''	20° 22' 33.93''	74
10	44° 47' 10.40''	20° 23' 33.13''	73
12	44° 47' 19.20''	20° 23' 48.77''	72
28	44° 46' 57.54''	20° 23' 26.45''	70

reference velocity tracking of than fuzzy regulator. Regarding criterion on keeping the reference flight altitude better results are achieved by implementing BSM and PID techniques, too.

Some characteristic simulation results concerning precision of trajectory tracking, keeping reference flight speed and actual motor (rotor) speed as control variable are presented in Figs. 10 and 11. One of the drawbacks of implementation the backstepping controller regards to anisotropic operation of quadcopter motors Fig. 12 that have rather pronounced oscillation of rotor speeds.

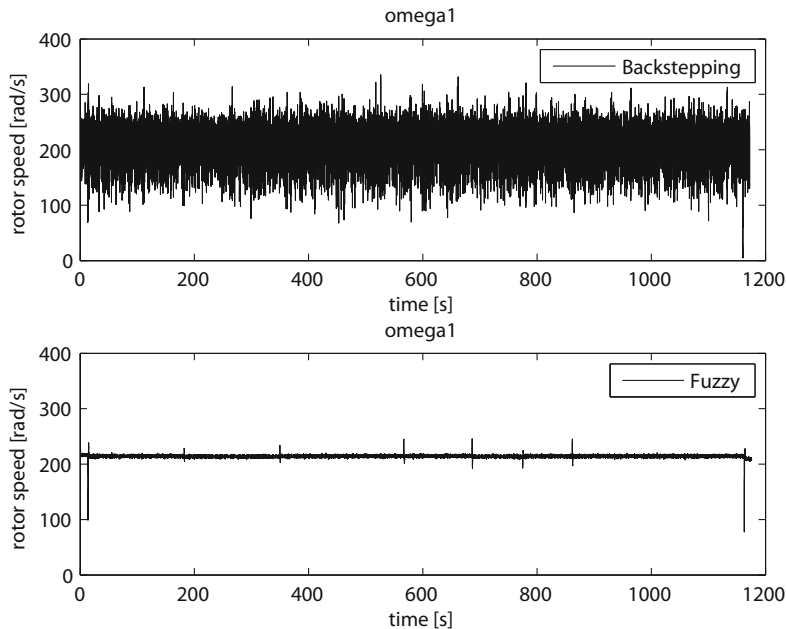


Fig. 12 Rotor speed as control variable obtained at the 1st motor of quadcopter

5 Conclusion

The paper regards to development of appropriate benchmarking and qualitative evaluation procedures dedicated to exploration, analysis and validation of flight controller performances of quadcopter UAVs. The system benchmarking represents inexpensive and no risky procedure for valuable assessment and evaluation of the control quality of the UAV systems. Because of that it is of great interest to set up appropriate benchmark simulation procedures to be accomplished before implementation of the chosen control algorithm with real microcopters. Two objective benchmark simulation tests are proposed in the paper. One indoor test, capable for exploration of dynamic flight scenarios and another outdoor waypoint navigation and trajectory tracking test are simulated. Three controllers (PID regulator, Backstepping and Fuzzy controller) as typical representatives of linear/non-linear and model-based/knowledge-based control techniques are validated through several closed-loop simulation tests. Based on a qualitative analysis of the obtained simulation results the Backstepping controller was identified as the best flight controller solution in this case. In spite of that, it has a drawback that regards to anisotropic operation of quadcopter motors that leads towards potential damaging of actuators over longer exploitation and worse energy efficiency. The PID regulator has certain advantages compared to the Backstapping and FLC, regarding to energy efficiency

and precision of reference velocity tracking. Concerning robustness to the internal and external perturbations, the Backstepping controller ensures better characteristics than two concurrent techniques. Generally spoken, existence of perturbations degrades the control system performances in all cases and in that sense need additional compensation. Proposed benchmark and evaluation procedure, described in the paper, can be usefully implemented in evaluation of other control methods in the same way, too. The proposed benchmarking procedure ensures equal conditions for testing and validation of different control architectures of such kind dynamic systems. It enables designer to bring valuable conclusions in the phase of controller development before performing tests with real system and in real exploitation conditions. Further research leads to combining (hybridization) of different types of control algorithms in order to minimize potential drawbacks of the particular techniques and to enhance their existing advantages.

Acknowledgements. This project is supported by Ministry of Science and Education of Republic Serbia under the grants TR-35003 and III-44008 and partially by the TÁMOP-4.2.2/08/1/2008-0008 program of the Hungarian National Development Agency.

References

1. Dzul, A., Castillo, P., Lozano, R.: Real-time stabilization and tracking of a four-rotor mini rotorcraft. *IEEE Transaction on Control System Technology* 12(4), 510–516 (2004)
2. Lozano, R., Castillo, P., Dzul, A.: Stabilization of a mini rotorcraft having four rotors. In: *Proceedings of 2004 IEEE/RSJ International Conference on Intelligent Robots and Systems*, Sendai, Japan, pp. 2693–2698 (2004)
3. Palomino, A., Salazar-Cruz, S., Lozano, R.: Trajectory tracking for a four rotor mini-aircraft. In: *Proceedings of the 44th IEEE Conference on Decision and Control, and the European Control Conference 2005*, Sevilla, Spain, pp. 2505–2510 (2005)
4. Noth, A., Bouabdallah, A., Siegwart, R.: Pid vs lq control techniques applied to an indoor micro quadrotor. In: *Proceedings of the 2004 IEEE/RSJ International Conference on Intelligent Robots and Systems*, vol. 3, pp. 2451–2456 (2004)
5. Tayebi, A., McGilvray, S.: Attitude stabilization of a vtol quadrotor aircraft. *IEEE Transaction on Control System Technology* 14(3), 562–571 (2006)
6. Fradkov, A., Andrievsky, B., Peaucelle, D.: Adaptive control experiments for laas helicopter benchmark, pp. 760–765 (2005)
7. Morel, Y., Leonessa, A.: Direct adaptive tracking control of quadrotor aerial vehicles. In: *Florida Conference on Recent Advances in Robotics*, pp. 1–6 (2006)
8. Lozano, R., Castillo, P., Dzul, A.: Stabilization of a mini rotorcraft with four rotors. *IEEE Control Systems Magazine*, 45–55 (2005)
9. Turczi, A.: Flight Control System of an Experimental Unmanned Quad-Rotor Helicopter. In: *Proceedings of the 10th International Symposium of Hungarian Researchers on Computational Intelligence and Informatics* (2009)
10. Madani, T., Benallegue, A.: Backstepping control for a quadrotor helicopter. In: *Proceedings of 2006 IEEE/RSJ International Conference on Intelligent Robots and Systems*, pp. 3255–3260 (2006)

11. Mokhtari, A., Benallegue, A.: Dynamic feedback controller of euler angles and wind parameters estimation for a quadrotor unmanned aerial vehicle. In: *Proceedings of the 2004 IEEE International Conference on Robotics and Automation*, pp. 2359–2366 (2004)
12. Benallegue, A., Mister, V., M'Sirdi, N.K.: Exact linearization and noninteracting control of a 4 rotors helicopter via dynamic feedback. In: *IEEE International Workshop on Robot and Human Interactive Communication*, pp. 586–593 (2001)
13. Valenti, M., Tournier, G.P., How, J.P.: Estimation and control of a quadrotor vehicle using monocular vision and moire patterns. In: *AIAA Guidance, Navigation, and Control Conference and Exhibit* (2006)
14. Hamel, T., Metni, N., Derkx, F.: Visual tracking control of aerial robotic systems with adaptive depth estimation. In: *Proceedings of the 44th IEEE Conference on Decision and Control, and the European Control Conference*, pp. 6078–6084 (2005)
15. Ostrowski, J.P., Altug, E., Taylor, C.J.: Quadrotor control using dual camera visual feedback. In: *Proceedings of the 2003 IEEE International Conference on Robotics and Automation*, pp. 4294–4299 (2003)
16. Earl, M.G., D'Andrea, R.: Real-time attitude estimation techniques applied to a four rotor helicopter. In: *43rd IEEE Conference on Decision and Control*, pp. 3956–3961 (2004)
17. Coza, C., Macnab, C.J.B.: A new robust adaptive-fuzzy control method applied to quadrotor helicopter stabilization (2006)
18. Tarbouchi, M., Dunfied, J., Labonte, G.: Neural network based control of a four rotor helicopter. In: *2004 IEEE International Conference on Industrial Technology*, pp. 1543–1548 (2004)
19. Jang, J.S., Waslander, S.L., Hoffmann, G.M., Tomlin, C.J.: Multi-agent quadrotor testbed control design: Integral sliding mode vs. reinforcement learning. In: *Proceedings of 2005 (IROS) IEEE/RSJ International Conference on Intelligent Robots and Systems*, pp. 3712–3717 (2005)
20. Hehn, M., Ritz, R., Andrea, R.: Performance benchmarking of quadrotor systems using time-optimal control. *Autonomous Robots*, 1–20 (2012), doi:10.1007/s10514-012-9282-3
21. Bresciani, T.: *Modelling, Identification and Control of a Quadrotor Helicopter*. MSc Dissertation, Department of Automatic Control, Lund University (2008)
22. Rodic, A., Mester, G.: The Modeling and imulation of an Autonomous Quad-Rotor Microcopper n a Virtual Outdoor Scenario. *Acta Polytechnica Hungarica* 8(4), 107–122 (2011)
23. Rodic, A., Mester, G.: Modeling and Simulation of Quad-rotor Dynamics and Spatial Navigation. In: *Proceedings of the SISY 2011, 9th IEEE International Symposium on Intelligent Systems and Informatics*, Subotica, Serbia, pp. 23–28 (2011), doi:10.1109/SISY.2011.6034325
24. Bouabdallah, S., Siegwart, R.: Backstepping and Sliding-mode Techniques Applied to an Indoor Micro Quadrotor. In: *Proceedings of the 2005 IEEE International Conference on Robotics and Automation ICRA 2005*, pp. 2247–2252 (2005)
25. Raza, S.A., Gueaieb, W.: *Intelligent Flight Control of an Autonomous Quadrotor*. In: Casolo, F. (ed.) *InTech* (2010) ISBN: 978-953-7619-55-8
26. Santos, M., Lopez, V., Morata, F.: Intelligent fuzzy controller of a quadrotor. In: *International Conference on Intelligent Systems and Knowledge Engineering, ISKE 2010*, pp. 141–146 (2010)
27. <http://www.google.com/earth/index.html>